Electrical and Mechanical Fully Coupled Theory and Experimental Verification of Rosen-Type Piezoelectric Transformers

Yu-Hsiang Hsu, Chih-Kung Lee, and Wen-Hsin Hsiao

***Abstract*—A piezoelectric transformer is a power transfer device that converts its input and output voltage as well as current by effectively using electrical and mechanical coupling effects of piezoelectric materials. Equivalent-circuit models, which are traditionally used to analyze piezoelectric transformers, merge each mechanical resonance effect into a series of ordinary differential equations. Because of using ordinary differential equations, equivalent circuit models are insufficient to reflect the mechanical behavior of piezoelectric plates. Electromechanically, fully coupled governing equations of Rosen-type piezoelectric transformers, which are partial differential equations in nature, can be derived to address the deficiencies of the equivalent circuit models. It can be shown that the modal actuator concept can be adopted to optimize the electromechanical coupling effect of the driving section once the added spatial domain design parameters are taken into account, which are three-dimensional spatial dependencies of electromechanical properties. The maximum power transfer condition for a Rosen-type piezoelectric transformer is detailed. Experimental results, which lead us to a series of new design rules, also are presented to prove the validity and effectiveness of the theoretical predictions.**

I. Introduction

Since the beginning of the 21st century, the worldwide trend of high-tech products has moved toward being more portable and possessing low profiles characterized by high energy density. Notebooks, cell phones, and personal digital assistants (PDA) are just some representative examples. Toward this trend, power supplies of high energy densities and low profiles are fast becoming one of the key technology components supporting these products. Because piezoelectric transformers possess merits such as having low profiles, high efficiencies, high energy densities, no electromagnetic interference, and having no potential for short circuiting hazardousness as compared to traditional electromagnetic transformers, they have been actively studied and are set to become one of the most important future power transfer devices [1]–[3]. The concept of placing a piezoelectric actuator and sensor together to function as a transformer was first conceived by Rosen in 1956 [4], [5]. His invention is shown in Fig. 1. As possessing high quality factor and thus high efficiency, a piezoelectric operating at a resonance mode can boost a low voltage energy source to a high energy source. Because a piezoelectric transformer is an electromechanical coupled device, it is proved and reported that its step-up ratio will reduce with a decreased load impedance. This characteristic matches perfectly with cold cathode fluorescent lamp (CCFL) [2], [3], and it retrigger many research activities to study the physical characteristics and interfacing circuits of piezoelectric transformers in this line of applications [4]–[11].

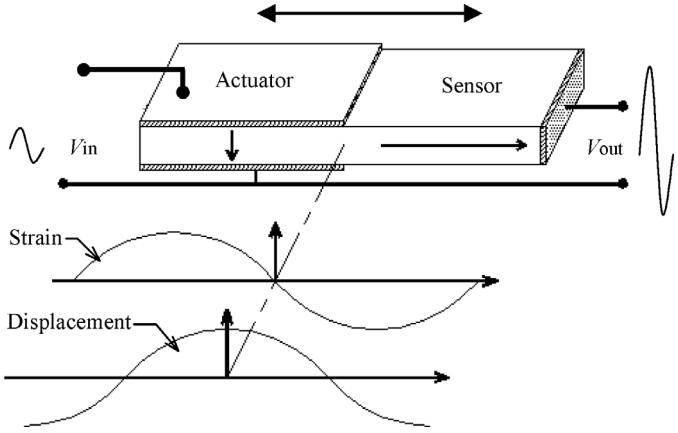

Fig. 1. Schematic of a Rosen-type piezoelectric transformer.

The driving circuit of previous traditional piezoelectric transformers was designed by taking the concept of using the piezoelectric transformer as a single resistor-inductor-capacitor (RLC) circuit resonance tank with inductors in the driving circuit. This fundamental thought is the basis of the various driving circuits developed for different applications [1]–[3], [12]. Nevertheless, it clearly can be demonstrated in this article that these traditional equivalent circuit approaches, which only adopt time as the independent variable and are thus an ordinary differen-

Manuscript received August 25, 2004; accepted February 6, 2005. The authors would like to acknowledge the continuous and generous financial support of this research from the National Science Council of Taiwan, R.O.C., and from AHEAD Optoelectronics, Inc., through Grants NSC 85-2622-E-002-017R, NSC 86-2622-E-002-023R, NSC 88-2218-E-002-005, and NSC 88-2622-E-002-001. The financial and material support of the AdvanceWave Technologies, Inc. is greatly appreciated as well. Appreciations also go to Eleceram Technology Co. Ltd. for providing us with the piezoelectric transformers used in this research work.

Y.-H. Hsu is with the Institute of Applied Mechanics, National Taiwan University, Taipei, Taiwan 106, Republic of China.

C.-K. Lee is with the Institute of Applied Mechanics as well as the Department of Engineering Science and Ocean Engineering, National Taiwan University, Taipei, Taiwan 106, Republic of China (e-mail: cklee@mems.iam.ntu.edu.tw).

W.-H. Hsiao is with AdvanceWave Technologies, Inc., Taipei, Taiwan 106, Republic of China.

0885–3010/$20.00 © 2005 IEEE

Authorized licensed use limited to: National Taiwan University. Downloaded on December 24, 2008 at 21:43 from IEEE Xplore. Restrictions apply.

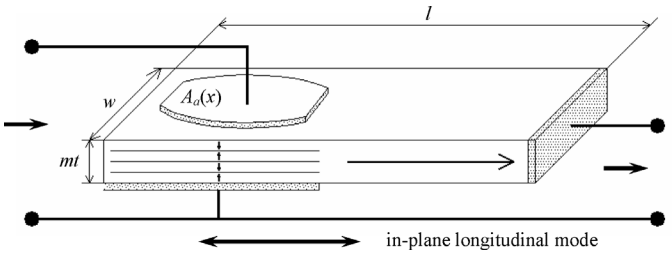

Fig. 2. Schematic of a multilayered Rosen-type piezoelectric transformer with in-plane longitudinal vibration.

tial equation. These equivalent circuit models neglect that the electromechanical coupling vibration of piezoelectric transformers can be modeled only spatially and are a time-dependent, partial differential equation. More specifically, the equivalent circuit model can describe only the vibration of a piezoelectric transformer for a specific mode and cannot express the interactions among the different modes. In other words, the piezoelectric transformer must be perceived as a mechanical resonance device with space and time dependency, and it is influenced by both electrical and mechanical boundary conditions [13], [14]. The fully coupled field equations of a surface-to-surface piezoelectric transformer based on the nature of partial differential equations was first derived by authors [15], which was a piezoelectric transformer with identical poling directions for actuator and sensor. In this article, fully coupled field equations of a Rosen-type piezoelectric transformer, which has poling directions of actuator and sensor orthogonal to each other, will be detailed to show the characteristics of these devices. It clearly will be demonstrated in this article that the actuator and sensor orientations lead to optimal electromechanical matching characteristics for CCFL applications. To optimize the energy conversion and transformation, fully coupled field equations handling both temporal and spatial characteristics are essential and necessary. The physical operating characteristics of the piezoelectric transformer, both mechanical and electrical parts, will be examined in detail by using these newly derived field equations. The modal actuator concept [16] also will be introduced to optimize the power transfer from an electrical energy to mechanical vibration at the actuating area [15]. Both theoretical derivations and experimental results related to the modal strain, actuating-based piezoelectric transformers are detailed.

II. One-Dimensional Governing Equation of Piezoelectric Plates

A Rosen-type piezoelectric transformer is a structure joined by an actuator and a sensor and is operated at a specific resonant frequency of the joint structure. Fig. 2 is a schematic of a multilayered, Rosen-type piezoelectric transformer, which clearly indicates that the poling directions of the driving and sensing section are not the same. The poling direction and the orientation of the coordinates

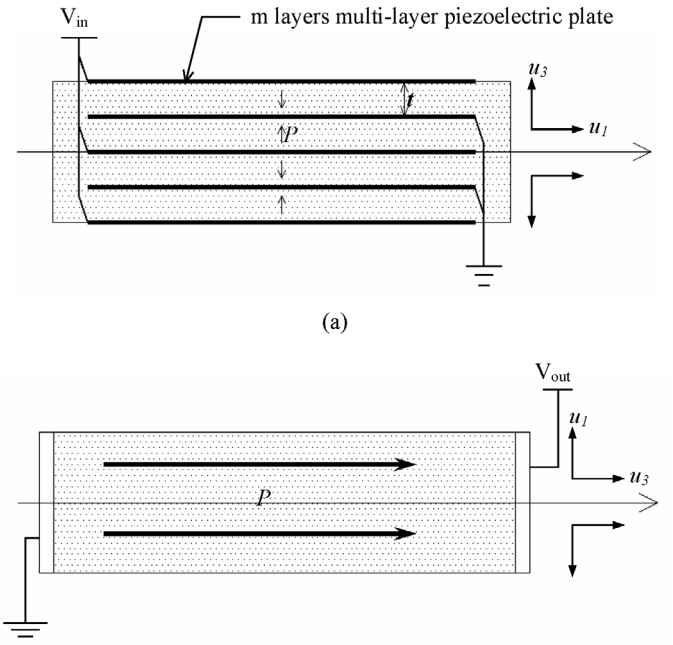

Fig. 3. Schematic of piezoelectric plates of piezoelectric transformers: (a) actuator and (b) sensor.

of the actuator and sensor are shown in Figs. 3(a) and (b), respectively. Thus, the electromechanical coupling coefficients adopted to model these two sections must be different. Because the Posen-type piezoelectric transformer is a slender plate, the one-dimensional field equations of piezoelectric plates are derived based on the following assumptions: the length l of a piezoelectric plate of interest is much longer when compared to its width w; the wavelength along the used longitudinal structure vibration will not be significantly influenced by the boundaries along the width; the thickness of the piezoelectric plate is much thinner than its width w; the thickness of the electrodes is much thinner than the thickness of the piezoelectric plate t; the displacement fields are symmetric with respect to its neutral plane; and its boundary conditions are traction-free for the joint structure. Thus, reduced governing equations and constitutive equations for the actuator and the sensor can be written as the following two sets of equations, respectively, [14], [15]:

$$c_{11}^{E}\tilde{u}_{1,11} - e_{31}mV_3^{in} = \rho\ddot{\tilde{u}}_1, \tag{1a}$$

$$\begin{cases} \tilde{T}_1 = c_{11}^{E}\tilde{u}_{1,1} - me_{31}(V_3) \\ mt\tilde{D}_3 = e_{31}\tilde{u}_{1,1} + m\varepsilon_{33}^{s}(V_3) \end{cases}, \tag{1b}$$

and

$$\left(c_{33}^{E} + \frac{e_{33}^2}{\varepsilon_{33}^{s}}\right)\tilde{u}_{3,33} = \rho\ddot{\tilde{u}}_3, \tag{2a}$$

$$\begin{cases} \tilde{T}_3 = c_{33}^{E}\tilde{u}_{3,3} - e_{33}\left(\tilde{E}_3\right) \\ \tilde{D}_3 = e_{33}\tilde{u}_{3,3} + \varepsilon_{33}^{s}\left(\tilde{E}_3\right) \end{cases}, \tag{2b}$$

Authorized licensed use limited to: National Taiwan University. Downloaded on December 24, 2008 at 21:43 from IEEE Xplore. Restrictions apply.

where $u_{i,j}$ and $u_{i,jj}$ are the first and second direction derivatives with respect to the j^{th} direction for displacement along the i^{th} direction, T represent stress, D and E represent electric displacement and electrical field, c_{11} and c_{33} are the elastic compliance constants, ε is the permittivity constant, e_{31} and e_{33} are the piezoelectric stress constants, superscripts S and E indicate that the S and E fields remain constants, V is the applied voltage, and the $\sim$ sign indicates that the physical quantity is integrated along the thickness direction, which is different for the two types of piezoelectric plates shown in Figs. 3(a) and (b). It should be mentioned that the piezoelectric effect serves as an inhomogeneous term in the governing equation of the actuator in (1a) and stiffens the elastic constant of the governing equation for the sensor represented by (2a) [16]. The relationship between the material constants yields that the equivalent elastic constant $c_{33}^E + e_{33}^2/\varepsilon_{33}^s$ in (2a) equals to c_{33}^D [14]. Changing the subscript 3 of the sensor displacement field u_3 to 1, and taking the displacement fields of the actuator and sensor as a summation of the normal modes, leads to the displacement field [17]:

$$\tilde{u}_1(x_1,t) = \sum_{i=1}^{\infty} A_i^{\alpha}(t)\phi_i^{\alpha}(x_1), \tag{3}$$

where the superscript α is a for the actuator and s for the sensor. It should be noted that orthogonal properties exist between the spatial functions $\phi_i^{\alpha}(x)$. Substituting (3) into the governing equation, and taking the volume integral with respect to $\phi_i^{\alpha}(x)$, the governing equation of a one-dimensional piezoelectric plate can be transferred into infinite sets of ordinary differential equations as follows [17]:

$$\sum_{i=1}^{\infty} \frac{d^2 A_i^{\alpha}(t)}{dt^2} + \frac{c_{\beta\beta}^{\gamma}(k_i^{\alpha})^2}{\rho} A_i^{\alpha}(t) = r_i^{\alpha}(t), \tag{4}$$

and

$$r_i^{\alpha} = -\frac{e_{31}}{\rho} m V_{3a}^{in} \int_0^{l_1} A_a'(x)\phi_i^a(x)dx + \frac{c_{11}^E}{\rho}\left[\frac{\partial\tilde{u}(l_1,t)}{\partial x}\phi_i^{\alpha}(l_1) - \frac{\partial\tilde{u}(0,t)}{\partial x}\phi_i^{\alpha}(0)\right], \tag{5a}$$

$$r_i^s(t) = \frac{c_{33}^D}{\rho}\left[\frac{\partial\tilde{u}(l,t)}{\partial x}\phi_i^s(l) - \frac{\partial\tilde{u}(l_1,t)}{\partial x}\phi_i^s(l_1)\right], \tag{5b}$$

where k_i^{α} is the wavenumber, l_1 is the location of the adjoining point between the actuator and sensor, subscript β and superscript γ are 1 and E for the actuator, as well as 3 and D for the sensor. Note that the driving voltage V_3^{in} can be rewritten as $V_{3a}^{in}A_a(x)$ to express the effect of the electrode shape. Because the piezoelectric transformer operates at the resonant frequency of its adjoined structure configuration, its time-varying functions $A_i^a(t)$ and $A_i^s(t)$ will be identical. In addition, the resonant frequency will be the same, i.e., $c_{11}^E(k_i^a)^2/\rho = c_{33}^D(k_i^s)^2/\rho$. The wavelength of sensor λ_i^s is thus equivalent to $(c_{33}^D/c_{11}^E)^{1/2}\lambda_i^a$. This relationship is identical to the one proposed by Lin in 1997 [1]. The sensor's governing equation can be merged into the actuator by setting an equivalent length of sensor l_s to $(c_{33}^D/c_{11}^E)^{1/2}(l-l_1)$, and the equivalent length of the piezoelectric transformer as l_p. Thus, the governing equation for the i^{th} mode is:

$$\frac{d^2 A_i(t)}{dt^2} + \frac{c_{11}^E(k_i^{\alpha})^2}{\rho}A_i(t) = -\frac{e_{31}}{\rho} m V_{3a}^{in}\int_0^{l_1} A_a'(x)\phi_i^a(x)dx + B(t), \tag{6}$$

where

$$B(t) = \frac{c_{11}^E}{\rho}\left[\frac{\partial\tilde{u}(l_1,t)}{\partial x}\phi_i^{\alpha}(l_1) - \frac{\partial\tilde{u}(0,t)}{\partial x}\phi_i^{\alpha}(0)\right] + \frac{c_{33}^D}{\rho}\left[\frac{\partial\tilde{u}(l_p,t)}{\partial x}\phi_i^s(l_p) - \frac{\partial\tilde{u}(l_1,t)}{\partial x}\phi_i^s(l_1)\right], \tag{7}$$

is the boundary term of the piezoelectric transformer. Applying the continuity condition at the adjoining point (i.e., electrical potential, electrical displacement, stress, and displacement are identical at both sides of the adjoining point [13]) leads to the boundary term at l_1 of the actuator and sensor in which they cancel out each other. However, the mechanical boundary conditions of the piezoelectric transformer in Fig. 2 are traction-free at the boundaries. The governing equation of a Rosen-type piezoelectric transformer becomes:

$$\frac{d^2 A_i(t)}{dt^2} + \frac{c_{11}^E(k_i^{\alpha})^2}{\rho}A_i(t) = -\frac{e_{31}}{\rho} m V_{3a}^{in}\int_0^{l_1} A_a'(x)\phi_i^a(x)dx + \frac{e_{33}}{\rho\epsilon_{33}^s}\tilde{D}_3(l_p,t)\phi_i^s(l_p). \tag{8}$$

It should be noted that the boundary terms of the actuator and sensor are different as they are governed by different governing equations. From (5a) and Fig. 2 we can see that the piezoelectric effect acts as a distributed force exerted through electrode $A_a(x)$ to the actuator portion of the piezoelectric plate and where as such the boundary term is zero. However, the output of the sensor side located at the right boundary (Fig. 2) and the load impedance offers an additional electrical boundary condition to the piezoelectric transformer. In other words, the load impedance provides a clamping force at the boundary of the piezoelectric transformer [14]. It can be concluded that the electrical energy drives the piezoelectric transformer through the electrode $A_a(x)$ and appears as a distributed force. In addition, the load impedance sinks the mechanical energy needed from the surface charge $\tilde{D}_3(l_p)$ as a boundary force. It should be noted that the driving voltages of the piezoelectric transformer are weighed by their surface electrodes $A_a(x)$. Thus, choosing the shape of the actuator electrode offers an opportunity to tailor the electromechanical coupling effect between the driving circuit and actuator [14]. It can be shown that the concept of a modal actuator is applicable to an actuator design [16].

Authorized licensed use limited to: National Taiwan University. Downloaded on December 24, 2008 at 21:43 from IEEE Xplore. Restrictions apply.

III. Operation of Piezoelectric Transformers

To understand the electromechanical coupling phenomenon of a power transfer between electrical and mechanical energies, the general solution of the Rosen-type piezoelectric transformer is derived. Taking an eigenfunction expansion of the governing equation of the Rosen-type piezoelectric transformer with boundary terms equal to zero leads to the following i^{th} eigen-function and eigenvalue:

$$\phi_i(x) = \sqrt{\frac{2}{l}}\cos(k_i x), \quad i = 1 \sim \infty, \tag{9}$$

and $k_i = i\pi/l$. Note that the multiplication constant $(2/l)^{1/2}$ is added to normalize the eigen-function such that the eigen-function integrates to one when the volume integral is performed. Substituting the eigen-function to (8) then taking the volume integral with respect to the i^{th} eigen-function, we obtain the displacement field of the Rosen-type piezoelectric transformer to be:

$$\tilde{u}_1(x,t) = \sum_{i=1}^{\infty} A_i(t)\phi_i(x) = \sum_{i=1}^{\infty} \frac{r_i}{(\omega_i^2 - \omega^2)}\phi_i(x), \tag{10}$$

where:

$$r_i = -\frac{e_{31}}{\rho} m V_{3a}^{in} \int_0^{l_1} A_a'(x)\phi_i(x)dx + \frac{e_{33}}{\rho\varepsilon_{33}^s}\tilde{D}_3(l_p,t)\phi_i^s(l_p), \tag{11}$$

and $\omega_i = \left(c_{11}^E k_i^2/\rho\right)^{1/2}$ is the i^{th} resonant frequency of the piezoelectric plate. Taking the surface integral with respect to the actuator electrode (1b) then performing a volume integral with the actuator portion as the integration domain leads to:

$$\begin{aligned}\int_0^l (mt\tilde{D}_{3a}^{in})A_a(x)dx &= \int_0^l (e_{31}\tilde{u}_{1,1})\,A_a(x)dx \\ &\quad + \int_0^l \left(\varepsilon_{33}^s m V_{3a}^{in}\right)A_a(x)dx, \end{aligned} \tag{12a}$$

$$\begin{aligned}\int_0^l (\tilde{D}_3)wdx &= \int_0^l (e_{33}\tilde{u}_{3,3})\,wdx \\ &\quad + \int_0^l \left(\varepsilon_{33}^s \tilde{E}_3\right)wdx, \end{aligned} \tag{12b}$$

where $\tilde{u}_{3,3}$ equals $\tilde{u}_{1,1}$ from (10). Because the constitutive equation represents a material property of piezoelectric materials, the charge displacement can be viewed as an internal property, i.e., when observing the charges generated on the electrodes, an opposite sign must be added to the results obtained from the volume integrals mentioned above. Furthermore, it has been mentioned that the driving current can spread into each layer of the multilayer actuator, and the supplied electrical field can be equally split across every layer. In other words, the supplied voltage will be equally split across every layer if the thickness of each layer is identical. Denoting the output voltages of the actuator and sensor as $V_{3a}^{in} = I_{3a}^{in}Z_e$ and $V_{3s}^{out} = I_{3s}^{out}Z_L$, respectively, and where Z_e and Z_L are the equivalent input impedance and external load impedance. Then (12a) and (12b) can be written as (12c) and (12d), respectively:

$$\begin{aligned} &mt\frac{I_{3a}^{in}}{j\omega} + \frac{e_{31}^2}{\rho}\frac{V_{3a}^{in}}{\omega_i^2 - \omega^2}\int_0^l A_a'(x)\phi_i(x)dx \int_0^l A_a(x)\phi_i'(x)dx \\ &\quad - m\varepsilon_{33}^s V_{3a}^{in}A_a(x) \\ &= \frac{e_{33}e_{31}}{\rho\varepsilon_{33}^s}\frac{I_{3s}^{out}}{j\omega}\frac{\phi_i(l_p)}{\omega_i^2 - \omega^2}\int_0^l A_a(x)\phi_i'(x)dx, \end{aligned} \tag{12c}$$

$$\begin{aligned} &\frac{I_{3s}^{out}(l_p - l_1)}{j\omega} - \frac{e_{33}^2}{\rho\varepsilon_{33}^s}\frac{I_{3s}^{out}}{j\omega}\frac{\phi_i(l_p)[\phi_i(l_p) - \phi_i(l_1)]}{\omega_i^2 - \omega^2} - \varepsilon_{33}^s V_{3s}^{out} \\ &= -V_{3a}^{in}\frac{e_{33}e_{31}}{\rho}\frac{[\phi_i(l_p) - \phi_i(l_1)]}{\omega_i^2 - \omega^2}\int_0^l A_a'(x)\phi_i(x)dx. \end{aligned} \tag{12d}$$

Express all current terms in terms of voltage and impedance and eliminate all voltage terms by combining (12d) in (12c) leads to the input impedance shown in (13) (see next page) where:

$$\omega_i'^2 = \omega_i^2 - m\frac{w}{t}\frac{e_{31}^2}{\rho C_a}\int_0^l A_a'(x)\phi_i(x)dx \int_0^l A_a(x)\phi_i'(x)dx, \tag{14}$$

ω_i is the resonant frequency, ω' is the antiresonant frequency, C_a is the static capacitance of the actuator, and C_s is the static capacitance of the sensor. Note that the damping effect of the piezoelectric transformer was added to (13). Considering the case in which no output electrodes exist, (13) shows the impedance of a piezoelectric plate as a function of its static capacitance C_a, the shape of the electrode $A_a(x)$, and the piezoelectric constants. However, for the case in which the output electrode is present, the input impedance of a piezoelectric transformer as shown in (13) becomes a function of the static capacitance of actuator C_a and sensor C_s; the shape of the actuator electrode $A_a(x)$; the piezoelectric constants that couple the mechanical and electrical quantities; and the load impedance Z_L of the sensor.

The transfer function of the Rosen-type piezoelectric transformer can be derived from (12d), in which all the output current terms were expressed in terms of output voltage terms, i.e., $I_{3s}^{out} = V_{3s}^{out}/Z_L$. The transfer function of the Rosen-type piezoelectric transformer then can be derived as (15) (see next page).

Note that the influence of the electromechanical property from the sensor and its load impedance are identical to the input impedance. However, the contribution of the sensor can be neglected at a high-load impedance Z_L as it does not sink the current out of the piezoelectric transformer. In such a case, the load impedance of the piezoelectric structure will not affect the electrical boundary condition; thus, the resonant characteristics of the piezoelectric transformer will be only a function of the mechanical properties. This result can be expressed by its transfer function at a high-load impedance as in (16) (see next page).

Authorized licensed use limited to: National Taiwan University. Downloaded on December 24, 2008 at 21:43 from IEEE Xplore. Restrictions apply.

$$Z_e = \sum_{i=1}^{\infty} \frac{-1}{j\omega c_a} \frac{\left(\omega_i^2 + 2\zeta(j\omega)\omega_i - \omega^2\right) - \dfrac{1}{(l_p - l_1)} \dfrac{1}{1 + j\omega Z_L C_s} \dfrac{e_{33}^2}{\rho\varepsilon_{33}^s} \phi_i(l_p)\left[\phi_i(l_p) - \phi_i(l_p)\right]}{\left(\omega_i'^2 + 2\zeta(j\omega)\omega_i' - \omega^2\right) - \dfrac{1}{(l_p - l_1)} \dfrac{1}{j\omega Z_L C_s} \dfrac{e_{33}^2}{\rho\varepsilon_{33}^s} \phi_i(l_p)\left[\phi_i(l_p) - \phi_i(l_1)\right]}. \tag{13}$$

$$\frac{V_{3s}^{out}}{V_{3a}^{in}} = \sum_{i=1}^{\infty} \frac{j\omega Z_L C_s}{1 + j\omega Z_L C_s} \frac{m\dfrac{w}{t}\dfrac{e_{31}e_{33}}{\rho C_s} \displaystyle\int_0^l A_a'(x)\phi_i(x)dx\left[\phi_i(l_p) - \phi_i(l_1)\right]}{\left(\omega_i^2 + 2\zeta(j\omega)\omega_i - \omega^2\right) - \dfrac{1}{(l_p - l_1)} \dfrac{1}{1 + j\omega Z_L C_s} \dfrac{e_{33}^2}{\rho\varepsilon_{33}^s} \phi_i(l_p)\left[\phi_i(l_p) - \phi_i(l_1)\right]}. \tag{15}$$

$$\frac{V_{3s}^{out}}{V_{3a}^{in}} = \sum_{i=1}^{\infty} \frac{j\omega Z_L C_s}{1 + j\omega Z_L C_s} \frac{m\dfrac{w}{t}\dfrac{e_{31}e_{33}}{\rho C_s} \displaystyle\int_0^l A_a'(x)\phi_i(x)dx\left[\phi_i(l_p) - \phi_i(l_1)\right]}{\left(\omega_i^2 + 2\zeta(j\omega)\omega_i - \omega^2\right)}. \tag{16}$$

Because the piezoelectric transformer is a mechanical resonant device, its quality factor can be as high as 1000 to 2000, depending on the PZT materials used. The step-up ratio thus can be in the range of several hundreds at an operating resonant frequency ω_i when a high-load impedance is present. When the load impedance Z_L starts to compete with the output impedance of the sensor's static capacitance $j\omega Z_L C_s$, the step-up ratio and the resonant frequency of the piezoelectric transformer will begin to drop as the load impedance sinks more mechanical resonance power. Mathematically, this drop can be understood by examining the low-pass filter formed by the load impedance and output static capacitance of the sensor as seen in (13) and (15). It should be noted that this low-pass filter $1/(1 + j\omega Z_L C_s)$ is weighted by the spatial properties of the sensor side. The weighted real part of this low-pass filter will reduce the resonant frequency of a piezoelectric transformer when the output impedance is closer to the output impedance. However, the imaginary part of this low-pass filter decreases the quality factor of the piezoelectric transformer by lowering the load impedance. Note that this phenomenon exists for both the input impedance and the transfer function shown in (13) and (15). By using the same materials constants and geometries of the Rosen-type piezoelectric transformer shown in Fig. 4, its theoretical simulation of the variation of the resonance and damping ratio with respect to the loading impedance Z_L are shown in Figs. 5(a) and (b). This schematic clearly demonstrated that the real part and imaging part of the underlined low-pass filter did reveal the influence of the loading impedance to the resonance effect. Physically, the stiffness of a piezoelectric material will soften at low-load impedances and stiffen at high-load impedances [14]. This phenomenon is also the underlying reason why piezoelectric transformers are the ideal driving circuits for lighting up a CCFL tube [1]. As was mentioned above, the load impedance influences both the resonant frequency and the quality factor of the piezoelectric transformer. In addition, a built-in, high-pass filter also influences the transfer function of the piezoelectric transformer. In the next section, the transfer function of a Rosen-type piezoelectric transformer operating at an optimal condition as a function of both the mechanical and electrical properties of the actuator and the sensor will be detailed.

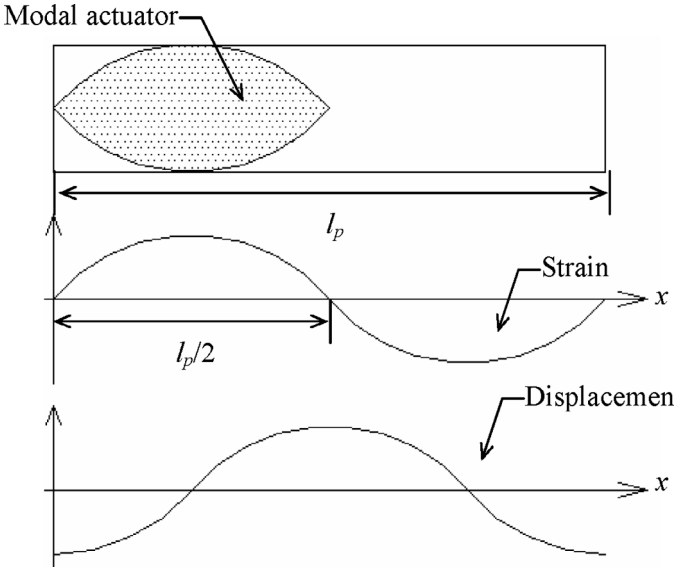

Fig. 4. Schematic of a modal driven Rosen-type piezoelectric transformer.

A. Optimized Power Transfer of Piezoelectric Transformers

A piezoelectric transformer is a power transfer device that uses a mechanical resonance effect to transfer a low-

Authorized licensed use limited to: National Taiwan University. Downloaded on December 24, 2008 at 21:43 from IEEE Xplore. Restrictions apply.

$$Z_e = \sum_{i=1}^{\infty} \frac{-1}{j\omega C_a} \frac{(\overline{\omega}_i^2 + 2\zeta'(j\omega)\overline{\omega}_i - \omega^2)}{(\overline{\omega}_i'^2 + 2\zeta'(j\omega)\overline{\omega}_i' - \omega^2)}, \tag{17a}$$

$$\frac{V_{3s}^{out}}{V_{3a}^{in}} = \sum_{i=1}^{\infty} \frac{j\omega Z_L C_s}{1 + j\omega Z_L C_s} \frac{m\frac{w}{t}\frac{e_{31}e_{31}}{\rho C_s}\int_0^l A_a'(x)\phi_i(x)dx\left[\phi_i(l_p) - \phi_i(l_1)\right]}{(\overline{\omega}_i^2 + 2\zeta'(j\omega)\overline{\omega}_i - \omega^2)}, \tag{17b}$$

where:

$$\overline{\omega}_i^2 = \omega_i^2 - \frac{1}{2}\frac{1}{(l_p - l_1)}\frac{e_{33}^2}{\rho\varepsilon_{33}^s}\phi_i(l_p)\left[\phi_i(l_p) - \phi_i(l_1)\right], \tag{18a}$$

$$\begin{aligned}\overline{\omega}_i'^2 = \omega_i^2 &- m\frac{w}{t}\frac{e_{31}^2}{\rho C_a}\int_0^l A_a' A_a'(x)\phi_i(x)dx\int_0^l A_a(x)\phi_i'(x)dx \\ &- \frac{1}{2}\frac{1}{(l_p - l_1)}\frac{e_{33}^2}{\rho\varepsilon_{33}^s}\phi_i(l_p)\left[\phi_i(l_p) - \phi_i(l_1)\right],\end{aligned} \tag{18b}$$

$$2\zeta'(j\omega)\overline{\overline{\omega}}i = 2\zeta(j\omega)\omega_i - \frac{1}{2}\frac{1}{(l_p - l_1)}\frac{e_{33}^2}{\rho\varepsilon_{33}^s}\phi_i(l_p)\left[\phi_i(l_p) - \phi_i(l_1)\right]. \tag{18c}$$

voltage power source to a high-voltage source. The optimal power transfer condition matches its output impedance to the load impedance [2], [3], [15]. That is, the output impedance of the piezoelectric transformer $|1/j\omega C_s|$ equals the load impedance Z_L at a resonant frequency. At this optimal power transfer condition, its input impedance and transfer function can be rewritten as (17) and (18) (see above).

Note that the load impedance lowers both the resonant and the antiresonant frequencies of the piezoelectric transformer while increasing the damping ratio (18a) and (18b). It should be mentioned again that a spatially weighted low-pass filter formed by an output static capacitance and load impedance contributes to this phenomenon. In other words, the vibration of a piezoelectric transformer operating at an optimal condition is a spatial and temporal function. This result clearly demonstrates that traditional equivalent circuits used for piezoelectric transformers cannot completely express its mechanical vibration, as the spatial information of the mechanical vibration is lost. Because the quality factor of a piezoelectric transformer is high, the additional damping effect incurred by the load term in (18c) becomes dominant at the resonant frequency. The step-up ratio of the piezoelectric transformer that operates at the i^{th} mode resonant frequency and at the optimal load condition will become:

$$\left|\frac{V_{3s}^{out}}{V_{3a}^{in}}\right| = \left|m\sqrt{2}\frac{w(l_p - l_1)e_{31}\varepsilon_{33}^s}{te_{33}C_s}\frac{\int_0^l A_a'(x)\phi_i(x)dx}{\phi_i(l_p)}\right|. \tag{19}$$

As the optimal power transfer condition requires that the output impedance of the piezoelectric transformer match the load impedance, the only remaining design parameter of piezoelectric transformer that can be used to tailor the step-up ratio is choosing the number of layers m of the multilayer actuator in (19). In summary, the optimal power transfer condition of a piezoelectric transformer requires matching its output static capacitance to its load impedance, and where the appropriate m layers of the multilayer actuator are chosen to meet the required step-up ratio. It should be noted that a high-pass filter, which is formed by a load impedance, and output static capacitance exists at the transfer function of the piezoelectric transformer. Under an optimal load condition, the corner frequency of this high-pass filter coincides with the operating resonant frequency, which leads to a 45° phase lead at the transfer function.

B. Modal Driven Rosen-Type Piezoelectric Transformer

Lee and Moon in 1990 [16], first invented the concept of a modal sensor and actuator. The underlying fundamental thought at that time was to use a shaped piezoelectric thin film to match one of the modal strains of the attached structure in order to overcome the spillover problem associated with the advancement of flexible structure control. The beauty of this modal sensor/actuator lies on using the orthogonal property between the eigen-functions to filter out the contributions from other modes, i.e., [15], [16]:

$$\int_0^l \phi_i(x)\phi_j(x)dx = \delta_{ij}, \tag{20}$$

where δ_{ij} equals 1 for $i = j$ and equals zero for $i \neq j$. Because the piezoelectric transformer operates at a specific resonant frequency, the modal actuator serves as the optimal design point to use the electromechanical coupling between the driving circuit and the mechanical vibration. The inhomogeneous term contributing to the governing equation of the actuator in (18) is:

$$-\frac{e_{31}}{\rho}mV_{3a}^{in}\int_0^{l_1} A_a'(x)\phi_i^a(x)dx, \tag{21}$$

Authorized licensed use limited to: National Taiwan University. Downloaded on December 24, 2008 at 21:43 from IEEE Xplore. Restrictions apply.

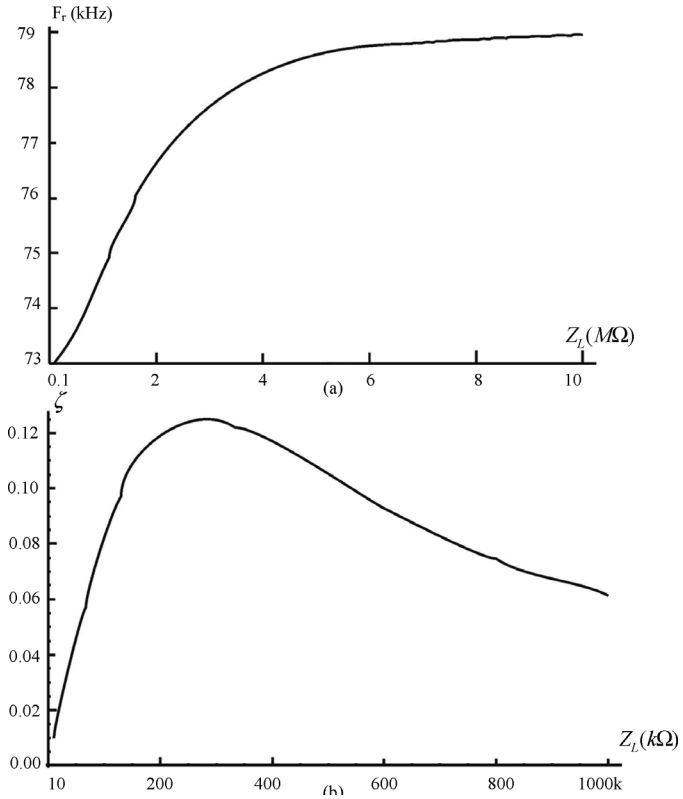

Fig. 5. Schematic of the influence of the low-pass filter $1/(1 + j\omega Z_L C_s)$, where (a) is the variation of the resonance frequency F_r with respect to the loading impedance Z_L, and (b) is the variation of the damping ratio ζ with respect to the loading impedance Z_L.

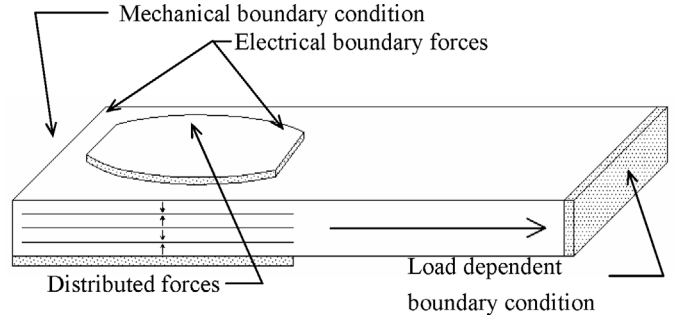

Fig. 6. Schematic of electromechanical coupled external forces of a Rosen-type piezoelectric transformer.

where the shape of the electrode $A_a(x)$ offers a weighting function to the eigen-function $\phi_i^a(x)$. The concept of a modal actuator then can be applied easily to the piezoelectric transformer. That is, the shape of the actuator equals to $d\phi_i^a(x)/dx$. Fig. 4 shows the top view of a Rosen-type piezoelectric transformer equipped with a mode-two actuator and operating in the second mode. In this case, the energy coupling between the driving circuit and mechanical part will be optimal. It should be mentioned that this modal actuator is actually a quasimodal actuator as only half of the modal actuator can be implemented on the Rosen-type piezoelectric transformer (see Fig. 6). More specifically, only a half cycle of the second modal strain can be matched. Thus, this quasimodal actuator cannot actually reach the requirements of the original modal actuator shown in (20), and thus cannot fully enjoy the advantages of modal selectivity. Nevertheless, this quasimodal actuator does match the strain distribution of the second mode, and thus has the ability to transfer all of the input energy to the resonant tank formed by the second mode. In this way, the power transfer efficiency from the electrical energy to the mechanical vibration will be optimal at the actuator section.

This design is significantly different from that of the traditional Rosen-type piezoelectric transformer, which has the actuator electrode $A_a(x)$ as $[H(x) - H(x - l_1)]$. The integration of (21) thus becomes:

$$\phi_i^a(0) - \phi_i^a(l_p). \tag{22}$$

This design matches the displacement field of the piezoelectric transformer (Fig. 4) and acts like an electrical boundary force applied at the piezoelectric transformer [15]. That is, the physical meaning of the weighting function of the electrode is a distributed force as the boundaries of the electrode offers electrical boundary forces. Fig. 7 summarizes the electromechanical coupled external forces of a Rosen-type piezoelectric transformer. It shows that the actuator offers a distributed force and two boundary forces, and the load condition serves as an electrical clamping boundary force to the piezoelectric transformer. In summary, the optimal requirement of a piezoelectric transformer is to match the load impedance to its output capacitance, and to choose m layers in the multilayer actuator with the corresponding modal actuator so as to achieve the desired step-up ratio. The coupling effect between the electrical and the mechanical energies can be further verified by the experiments in the next section.

IV. Experimental Setup

A 44-mm long by 6.5-mm wide by 2.2-mm thick single-layer, Rosen-type piezoelectric transformer made of PZT-8 (Fig. 6) was used to verify the theory derived above. To satisfy the derived, one-dimensional governing equation of the Rosen-type piezoelectric transformer shown in (8), the actuator and the sensor equations were merged together. With an attempt to make the equivalent length of sensor l_s equal to a half period of the second mode so as to implement a modal actuator at the actuator section that equals to $\left(c_{33}^D/c_{11}^E\right)^{1/2}(l - l_1)$, the length of the actuator and sensor used were 22.89 mm and 21.11 mm, respectively. The elastic constants of a PZT-8 were incorporated and $c_{11}^E = 13.7 \times 10^{10}$ N/m^2 and $c_{33}^D = 16.1 \times 10^{10}$ N/m^2 were adopted. The output capacitance was measured to be around 8 pF using an Agilent 4294A (Agilent Technologies, Inc., Palo Alto, CA) [18] impedance analyzer. The theoretical optimal load impedance thus was calculated to be about 272.526 kΩ, which is the impedance of the output capacitance around the second resonant frequency at

Authorized licensed use limited to: National Taiwan University. Downloaded on December 24, 2008 at 21:43 from IEEE Xplore. Restrictions apply.

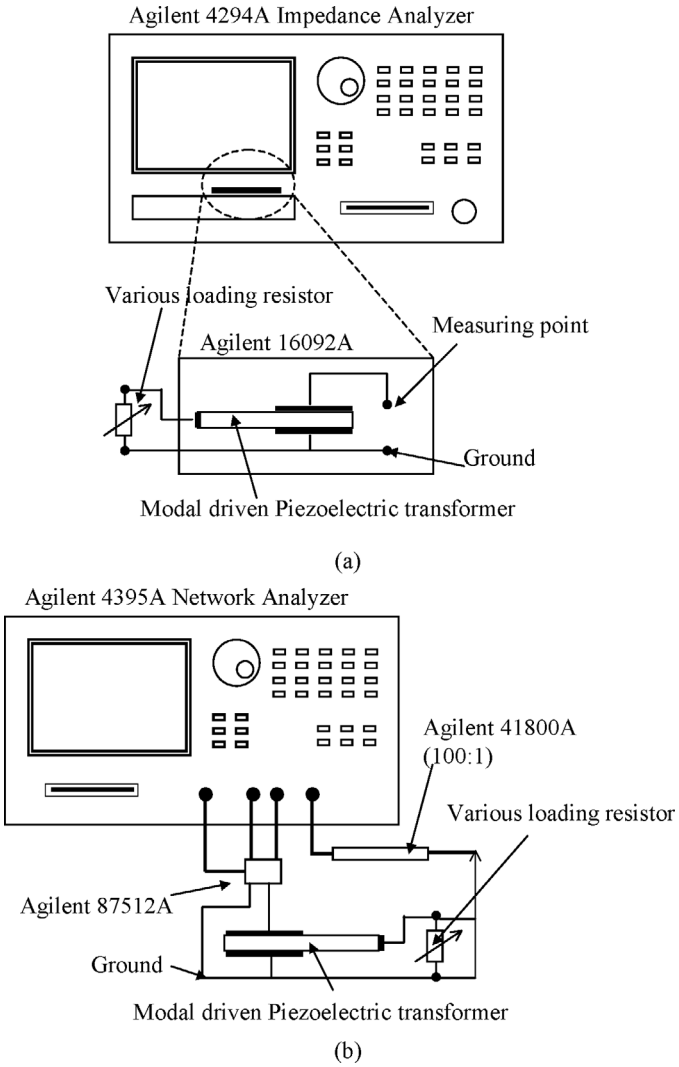

Fig. 7. Experimental setup measuring the input impedance (a) and transfer function (b) of a modal driven piezoelectric transformer.

73 kHz. Figs. 8(a) and (b) show the experimental set-up of measuring the input impedance and transfer function of this modal driven piezoelectric transformer and where the test results were recorded with different load resistors connected. Figs. 8 and 9 show the experimental results of the modal-driven, Rosen-type piezoelectric transformer as measured by Agilent 4395A network analyzers [19]. Note that the resonant frequencies of the input impedance and transfer function were reduced when the load impedance changed from an open to a short-circuit condition. However, the damping ratio increases as the load impedance moves away from infinity, i.e., from an open-circuit condition to closed-output impedance. The damping ratio was again reduced when the output impedance was further reduced from an optimal-load, impedance condition toward zero, i.e., a short-circuit condition. Fig. 10 shows the quality factor curve fitted around load impedance ranging from an open to a short-circuit condition. Note that the quality factor dropped to 12.27 at the maximum power transfer condition. This phenomenon agrees well with the theoret-

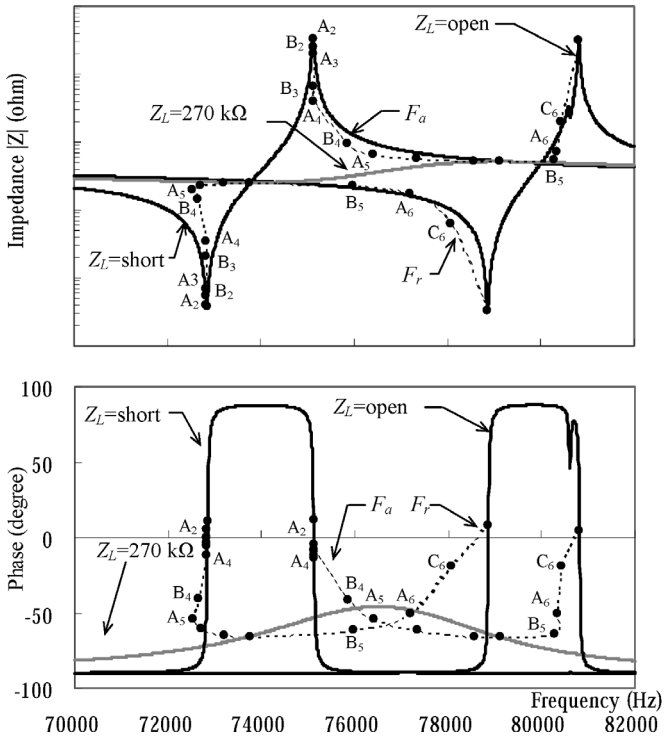

Fig. 8. Input impedance of a Rosen-type piezoelectric transfer with experimental results of an open circuit for output (dark line) and for an optimal power transfer (gray line) at 270 kΩ. The black dots are the experimental results of the impedance for the resonant frequency (F_r) with varying load impedances ranging from an open to a short-circuit condition of the output electrodes ($A_i = 10^i$, $B_i = 5.6 \times 10^i$, $C_i = 3.9 \times 10^i$).

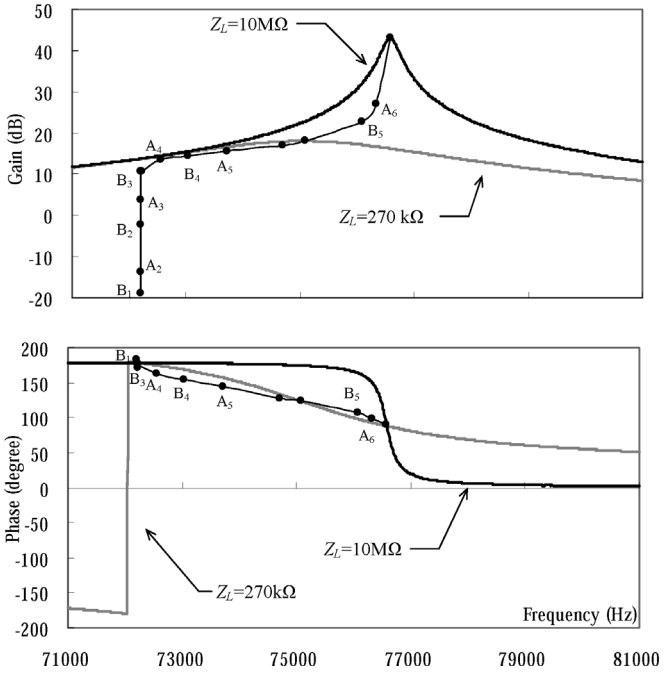

Fig. 9. Transfer function of a Rosen-type piezoelectric transfer with experimental results of an open circuit for output (dark line) and an optimal power transfer (gray line) at 270 kΩ, where (a) and (b) are the distributions of the gain and the phase with respect to frequency. The black dots are the experimental results of the impedance for the resonant frequency (F_r) with varying load impedances ranging from an open to a short circuit condition of the output electrodes.

Authorized licensed use limited to: National Taiwan University. Downloaded on December 24, 2008 at 21:43 from IEEE Xplore. Restrictions apply.

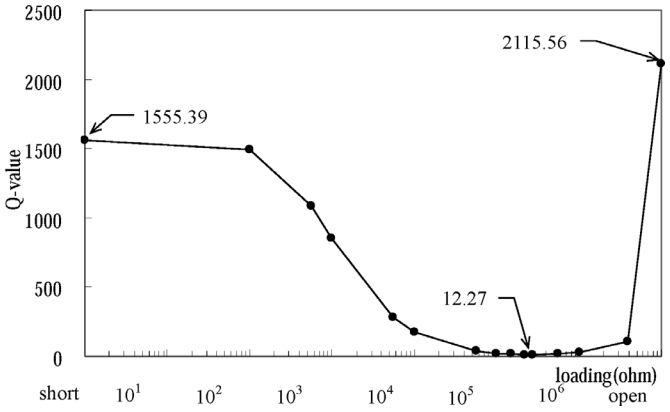

Fig. 10. Curve-fitted quality factor of input impedance showing different load impedances.

ical predictions as shown in (13) and (15). The low-pass filter formed by the load impedance and the output capacitance tailors the distribution of the input impedance and transfer function. As the load impedance is high with respect to the output impedance, the low-pass filter eliminates the influence of the load impedance. The resonant frequency of the piezoelectric transformer at this range remains almost the same as the load impedance is too high to sink current out of the piezoelectric transformer. That is, the piezoelectric transformer will not be affected by a clamped electrical boundary force, which is induced by the load impedance. As the load impedance approaches the output impedance, the output load reduces the system quality factor through the low-pass filter as shown (13). Note that the input impedance of the piezoelectric transformer increases from 33.5049 Ω to 2.53961 kΩ by the load impedance. The additional input impedance represents the impedance that sinks the sourcing power from the driving circuit. It also shows that the internal, mechanically induced power loss of the piezoelectric transformer is low due to its high mechanical quality factor.

To verify the concept of matching the output impedance to that of the load impedance of the piezoelectric transformer to arrive at the optimal condition for a maximum power transfer, an Avio infrared ray camera was used (Handy Thermo TVS-100 series, Nippon Avionics Co., Ltd., Tokyo, Japan). Figs. 11(a) and (b) compare the experimental results of a modal driven and traditional Rosen-type piezoelectric transformer. It is obvious from the experimental results that the sensor part of the piezoelectric transformer did not heat up, even when the input was set as high as 7 W at optimal conditions. Note also that the heat distribution of a modal driven and traditional piezoelectric transformer are significantly different. The hottest place of the modal actuator is at the nodal point of the actuator side, which is at the place at which the maximum strain will occur at the specific resonant frequency. Conversely, for traditional piezoelectric transformers, the hottest place is the area surrounding the boundaries of the actuator electrode. This clearly shows that modal actuators exert a distributed force, and traditional uniform electrodes offer only a boundary force. Under these conditions, the power delivered in and out of the piezoelectric transformer also was measured. It was found that the efficiency of the modal driven and traditional Rosen-type piezoelectric transformer was about 97.9% and 91.7%, respectively. In other words, the modal driven piezoelectric transformer was 6.2% better than that of the traditional type. It should be noted that the heat loss was reduced from 8.3% to 2.1%, which is a four times improvement in terms of heat loss. This significant heat loss improvement can be used to drastically improve transformer packaging. This experiment shows that the only way to force a piezoelectric transformer to operate at its optimal condition is to match its load impedance with its output capacitance and to use a modal actuator to match the electrical and mechanical energy transfer at the actuator.

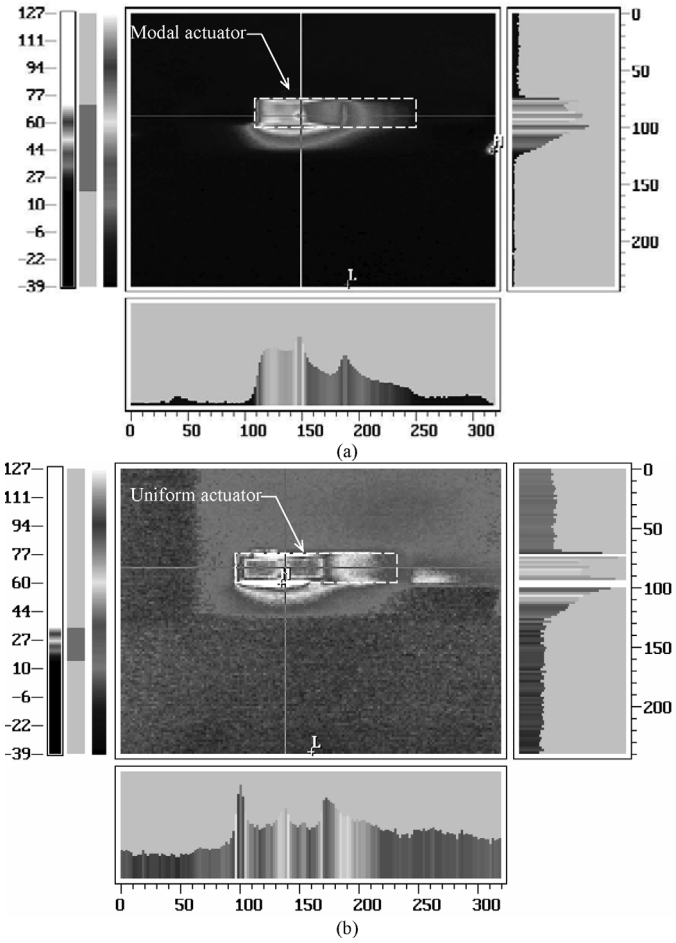

Fig. 11. Temperature field of (a) modal driven Rosen-type piezoelectric transformer (7 W) and (b) traditional Rosen-type piezoelectric transformer (8 W).

V. Conclusions

The field equations of a multilayer piezoelectric adjoined plate were derived to study the electromechanical

Authorized licensed use limited to: National Taiwan University. Downloaded on December 24, 2008 at 21:43 from IEEE Xplore. Restrictions apply.

coupling effects of piezoelectric transformers. The experimental results obtained on a modal driven and a traditional Rosen-type piezoelectric transformer made of PZT agree well with the theoretical predictions. It was shown that the vibration of a piezoelectric transformer is determined by: the distributed force exerted by the shaped actuator electrodes, the electrical boundary force at the boundaries of the actuator electrode, the mechanical boundary conditions, and the clamped electrical boundary force exerted by the load impedance. Based on these newly derived field equations, the optimal power transfer condition and its requirements on the load impedance of a piezoelectric transformer was determined. It was found that the piezoelectric transformer operating at an optimal power transfer condition can be designed by matching the load impedance with the output static capacitance, and choosing the appropriate m layers of a multilayer actuator to offer the desired step-up ratio as required by the system specifications. The results obtained lead to the conclusion that operating parameters associated with a piezoelectric transformer must be analyzed first by using the original partial differential equations as the field equations because both the temporal and spatial parameters are important. That is, the piezoelectric transformer must be analyzed as a fully electrical and mechanical coupled device in which its performance and system characteristics depend on both the mechanical and electrical properties. More specifically, the interface circuit will exert a very strong influence on the mechanical vibration through the effective surface electrodes. When field equations are considered, the electrical behavior of the applied voltage must be viewed as spatially dependent. Traditional equivalent circuit models neglect the influence of space information, and thus cannot be used to accurately predict the vibrational behavior of piezoelectric transformers. That is, even if an RLC resonance tank is used to represent its mechanical vibration, the equivalent passive components must be considered and viewed as dependent on the spatial variables such as $R(x)$, $L(x)$, and $C(x)$. To operate the piezoelectric transformer at an optimal condition both mechanically and electrically, we must: match the load impedance to the output impedance by computing the static output capacitance of the sensor area of the piezoelectric transformer, and adopt an effective surface electrode so that the strain distribution exerted by the actuator part of the piezoelectric transformer matches that of the specific mode of interest.

References

[1] C. Y. Lin, "Design and analysis of piezoelectric transformer converters," Ph.D. dissertation, Virginia Polytechnic Institute, Blacksburg, VA, 1997.

[2] J. Williams, "A Fourth Generation of LCD Backlight Technology," Application Note 65, Milpitas, CA: Linear Technology Corp., Nov. 1995.

[3] J. Williams, J. Phillips, and G. Vaughn, "Ultracompact LCD Backlight Inverters," Application Note 81, Milpitas, CA: Linear Technology Corp., Sep. 1999.

[4] C. A. Rosen, "Ceramic transformers and filters," in *Proc. Electric Comp. Symp.*, 1956, pp. 205–211.

[5] C. A. Rosen, "Piezoelectric transformers," U.S. Patent, No. 2830274, Apr. 1958.

[6] J. Kawai and B. Tagami, "Piezoelectric transformer and method for driving the same," U.S. Patent, No. 5365141, Nov. 1994.

[7] K. Kanayama and N. Maruko, "Piezoelectric transformer," U.S. Patent, No. 5701049, Dec. 1995.

[8] A. Tooru, "Piezoelectric transformer and power converting apparatus employing the same," U.S. Patent, No. 5751092, July 1996.

[9] Y. Tsuchiya, Y. Kagawa, N. Wakatsuki, and H. Okamura, "Finite element simulation of piezoelectric transformers," *IEEE Trans. Ultrason., Ferroelect., Freq. Contr.*, vol. 48, pp. 872–878, July 2001.

[10] K. Teranishi, H. Itoh, and S. Suzuki, "Dynamic behavior of light emissions generated by piezoelectric transformers," *IEEE Trans. Plasma Sci.*, vol. 30, pp. 122–123, Feb. 2002.

[11] A. M. Flynn and A. R. Sanders, "Fundamental limits on energy transfer and circuit considerations for piezoelectric transformers," *IEEE Trans. Power Electron.*, vol. 17, pp. 8–14, Jan. 2002.

[12] H. W. Katz, *Solid State Magnetic and Dielectric Devices*. New York: Wiley, 1959, pp. 94–126.

[13] H. F. Tiersten, *Linear Piezoelectric Plate Vibrations*. New York: Plenum, 1969.

[14] D. Royer and E. Dieulesaint, *Elastic Waves in Solids I*. New York: Springer, 1996.

[15] Y. H. Hsu, C. K. Lee, and W. H. Hsiao, "Optimizing piezoelectric transformer for maximum power transfer," *Smart Mater. Struct.*, vol. 12, pp. 373–383, June 2003.

[16] C. K. Lee and F. C. Moon, "Modal sensors/actuators," *Amer. Soc. Mech. Eng. J. Appl. Mech.*, vol. 57, pp. 434–441, June 1990.

[17] L. Meirovitch, *Element of Vibration*. Singapore: McGraw-Hill, 1986.

[18] Agilent Technologies Japan, Ltd., *Agilent 4294A Precision Impedance Analyzer Operation Manual*. Component Test PGU-Kobe 1-3-2, Murotani, Nishi-ku, Kobe-shi, Hyogo, 651-2241, Japan, Jan. 2001.

[19] Agilent Technologies Japan, Ltd., *Agilent 4395A Network/Spectrum/Impedance Analyzer Operation Manual*. Component Test PGU-Kobe 1-3-2, Murotani, Nishi-ku, Kobe-shi, Hyogo, 651-2241, Japan, Mar. 2000.

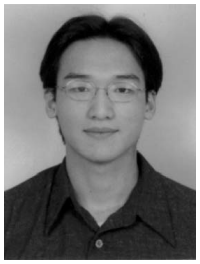

Yu-Hsiang Hsu received his Master of Science degree from the Institute of Applied Mechanics, National Taiwan University, Taipei, Taiwan. He has been involved in research topics related to flexible structure control, point sensor design, and piezoelectric transformer for the last six years at the Institute of Applied Mechanics of National Taiwan University. His research interests include piezoelectric sensors and actuators, power transfer, electro-mechanical coupled systems, etc.

Chih-Kung Lee received his Ph.D. degree from Cornell University, Ithaca, New York. He became a faculty member at the Institute of Applied Mechanics, National Taiwan University in 1994 after spending seven years as a Research Staff Member at IBM's Almaden Research Center in San Jose, California. He is also the director general of the Department of Engineering and Applied Science, National Science Council, Taiwan. He is also a Fellow of Institute of Physics. His research interests include design and development of optoelectronic systems, adaptive structures, distributed piezoelectric sensors and actuators, etc.

Authorized licensed use limited to: National Taiwan University. Downloaded on December 24, 2008 at 21:43 from IEEE Xplore. Restrictions apply.

Wen-Hsin Hsiao received her Master of Science degree from the Institute of Applied Mechanics, National Taiwan University, Taipei, Taiwan in 2000. She is now working as a senior engineer and project manager in AdvanceWave Tech. Inc., Taipei, Taiwan. Her research interests include flexible structure control, piezoelectric transformer, and electromechanical coupled systems, etc.

Authorized licensed use limited to: National Taiwan University. Downloaded on December 24, 2008 at 21:43 from IEEE Xplore. Restrictions apply.